17th World Conference on Earthquake Engineering, 17WCEE
Sendai, Japan - September 27th to October 2nd, 2021

RELATION BETWEEN STRENGTH DETERIORATION BEHAVIOR AND UNLOADING STIFFNESS OF SQUARE CFT COLUMNS

T. Susuki[(1)], M. Kido[(2)]

[(1)] *Graduate student, Graduate school of the University of Kitakyushu, b0mbb011@eng.kitakyu-u.ac.jp*
[(2)] *Associate Professor, The University of Kitakyushu, kido-m@kitakyu-u.ac.jp*

Abstract

A normal-trilinear model is generally used to represent the structural behavior of concrete-filled steel tubular (CFT) columns. Studies focusing on the hysteresis performance of CFT columns have shown the effects of axial force ratio and width–thickness ratio on the relationship between lateral drift and residual angles. CFT columns are popular structural elements in super-high-rise office buildings in Japan; however, there are still concerns about their performance under long-period ground motion, which is generated by earthquakes in the Nankai Trough. Previous work presented the experimental study of square CFT columns subjected to lateral cyclic load under constant rotation angles, simulating the effect of long-period ground motion. From this study, the strength deterioration behavior of the tested columns was observed. The results of the experimental study showed that the lateral load of the CFT columns decreased as the axial force ratio and amplitude of rotation angle increased. Furthermore, the relationship between lateral load and rotation angle changed as the number of cycles increased. The obtained results suggest that unloading stiffness decreases while the residual rotation angle increases together with the strength deterioration. These results are fundamental to support structural design processes of CFT columns and improve our understanding of the relationship between unloading stiffness or residual rotation angle and strength deterioration. This study focuses on the discussion of the relationship between the unloading stiffness and strength deterioration behavior of square CFT columns, as well as of the effects of the axial force ratio.

The number of specimens for this experiment consisted of 31 specimens of a steel square hollow section filled with concrete. The experimental parameters considered were the axial force ratio, width–thickness ratio, effective length-to-section depth ratio, rotation angle, status of concrete filling, and the strength of the steel tube. After unloading each cycle of the specimens, the residual rotation angle, R_r, was obtained from the lateral load and rotation angle relationship. The unloading stiffness, K_r, of the column was defined as the slope of a straight line between the displacement reversal point (experienced rotation angle R_0) and the point after unloading; both values were obtained from the lateral load and rotation angle relationship. Limit cycles indicating the reduction of lateral load by 95%, 90%, 85% and 80%, $N_{95\%}$, $N_{90\%}$, $N_{85\%}$, $N_{80\%}$, were defined as an index for exhibiting the performance against strength deterioration of CFT columns.

The initial lateral stiffness, K_{exp}, obtained from the experimental results was smaller than the elastic lateral stiffness, K_e, and the ratio of lateral stiffness to elastic stiffness K_{exp}/K_e varied from 0.60 to 1.01 with one exception. Besides, except when the axial force ratio, *n,* was equal to 0.5 or more, the difference between the initial lateral stiffness and unloading stiffness remained within 10% until the limit cycle, $N_{90\%}$, was reached.

The ratio between R_r and R_0 was defined as the residual deformation rate, *r*. The value of *r* increased as the axial force ratio increased. Furthermore, considering the limit cycles, the value of *r* increased in the following order: $N_{95\%}$, $N_{90\%}$, $N_{85\%}$, and $N_{80\%}$.

Keywords: Steel-concrete structure, Long-period ground motion, Lateral Stiffness, Residual rotation angle

1. Introduction

Hysteresis characteristics of concrete filled steel tubular columns (CFT columns) shown in Architectural Institute of Japan's (AIJ) recommendation for design and construction of concrete filled steel tubular structures (referred as Recommendations for CFT Structures) [1] is a normal trilinear model. Factors such as diameter-thickness ratio, width-thickness ratio, axial force ratio, buckling length-cross section ratio, etc. affects the hysteresis rule of CFT columns. If hysteresis characteristics is formulated considering these factors, the structural behavior of CFT structures can be predict more precisely. As a study related to a

skeleton curve of CFT columns, one of the authors have studied the initial lateral stiffness of CFT columns subjected to lateral force under constant axial load [2, 3]. Comparing with the elastic lateral stiffness and the secant stiffness obtained by connecting the short-term allowable strength, which is shown in Recommendations for CFT Structures, and the origin on the lateral load and lateral displacement relationship were about 43% smaller at the minimum. In Ref. [4], a method for evaluating the hysteresis characteristics of CFT columns is proposed by superposing the skeleton curves of square steel tubular columns and concrete columns. Regarding the initial lateral stiffness, the relationship between the initial lateral stiffness obtained from the experimental results of the CFT columns subjected to cyclic lateral load and the elastic lateral stiffness is examined in detail in Ref. [5].

Regarding the hysteresis rule, the unloading stiffness becomes an issue. In addition, large residual rotation angle can remain in some buildings after the huge earthquake due to yielding, and residual deformation affects the repairability of buildings. For this reason, in Ref. [6], the effects of axial force ratio and width-thickness ratio on the relationship between the experienced rotation angle and residual one of square CFT columns obtained from the previous experimental study were shown. In addition, in Ref. [7], the skeleton curve shown in Recommendations for CFT Structures was compared with the lateral load and lateral displacement relationship obtained by the alternately repeated cyclic loading test with incremental displacement. Recent research on seismic motions demonstrated that long-period earthquake ground motions may affect super-high-rise buildings and seismic isolation buildings located on large sedimentary plains. From this background, the authors conducted a bending-shear experiments of square CFT columns under cyclic lateral load with constant axial force. And the effects of the axial force ratio, displacement amplitude, width-thickness ratio of steel tube, and strength of steel tube on strength deterioration behavior were clarified [8~10].

It is considered that the unloading stiffness and residual rotation angle also change as the strength deterioration. Therefore, clarifying the relationship between the strength deterioration behavior and the unloading stiffness and the residual rotation angle can be useful data for the structural design. The purposes of this study are to examine the relationship between the strength deterioration behavior of slender square CFT columns and the unloading stiffness and residual rotation angle, and to clarify the effect of the axial force ratio on these relationships. This study includes some part of the previous research [11].

2. Outline of the experimental study [9, 10]

2.1 Plan of the Experiment

The outline of the experiment used in this study is shown below. The load condition is a square CFT column that are subjected to lateral load Q under a constant axial force N and the columns is a cantilever type with one end fixed and another end free as shown as Fig.1. In Fig. 1, δ is a lateral displacement at free end, R is a rotation angle and L is a member length.

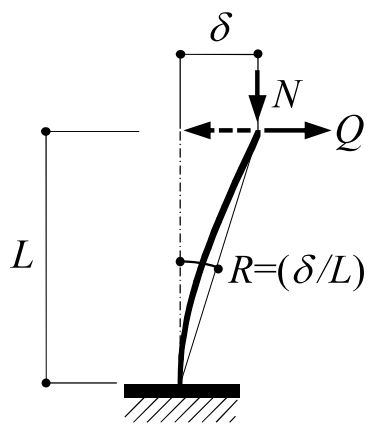

Fig. 1-Load condition

The experimental parameters and selected values are shown below.

1. Steel tube width-thickness ratio B/t_f: 25, 17
2. Effective length-depth of cross section ratio l_k/D: 20, 14
3. Axial force ratio n ($=N/N_0$, $N_0={}_sA\cdot{}_s\sigma_y+{}_cA\cdot{}_c\sigma_B$, ${}_sA$, ${}_cA$: the area of steel tube and concrete, ${}_s\sigma_y$: the yield strength of steel tube, ${}_c\sigma_B$: the compressive strength of concrete): 0.15, 0.3, 0.45, 0.6 (for B/t_f =25), 0.3, 0.5 (for B/t_f=17)
4. Displacement amplitude (Rotation angle) R_0: 0.5, 0.75, 1, 1.25, 1.5, 2, 2.5, 3% (for B/t_f =25), 1, 1.25, 1.5, 2% (for B/t_f=17)

Table 1-Specimen list

No.	Specimen	L(mm) (l_k/D)	B/t_f	n	R_0 (%)	${}_c\sigma_B$ (N/mm^2)	E_c (N/mm^2)	K_e (kN/rad)	S or CFT
1	S-LD14-n15R125	1050 (14)	25	0.15	1.25	-	-	6272	S
2	S-LD14-n15R15				1.5				
3	S-LD14-n30R1			0.3	1			6066	
4	S-LD14-n30R15				1.5				
5	S-LD14-n60R05			0.6	0.5			5651	
	S-LD14-n60R075				0.75				
6	S-LD14-n60R1				1				
7	LD14-n15R1			0.15	1	75.4	41199	9501	CFT
8	LD14-n15R15				1.5	76.0	41198	9499	
9	LD14-n30R1			0.3	1	75.7	39612	8905	
10	LD14-n30R15				1.5	70.9	38975	8883	
11	LD14-n45R1			0.45	1	76.6	41075	8550	
12	LD14-n45R125				1.25	77.5	43153	8711	
13	LD14-n60R075			0.6	0.75	75.6	42672	8267	
14	LD14-n60R1				1	77.3	41375	8160	
15	LD20-n45R15	1500 (20)		0.45	1.5	68.6	40442	3553	
16	LD20-n45R2				2	64.6	40666	3602	
17	LD20-n60R075			0.6	0.75	67.8	40666	3115	
18	S-LD20-n45R15			0.45	1.5	-	-	2604	S
19	S-LD20-n60R1			0.6	1	-	-	2384	
	S-LD20-n60R125				1.25				
20	LD14Bt17-n30R1	1050 (14)	17	0.3	1	68.1	39283	10172	CFT
21	LD14Bt17-n30R15				1.5	70.5	38854	10127	
22	LD14Bt17-n30R2				2	69.3	40788	10266	
23	S-LD14Bt17-n30R15				1.5	-	-	7932	S
24	LD14Bt17-n50R1			0.5	1	69.7	38702	9362	CFT
25	LD14Bt17-n50R125				1.25	68.1	39760	9445	
26	LD14Bt17-n50R15				1.5	67.7	39195	9416	
27	S-LD14Bt17-n50R125				1.25	-	-	7463	S
28	H-LD20-n30R2	1500 (20)	25	0.3	2	89.4	43678	4019	CFT
29	H-LD20-n30R3				3	89.6	42579	4017	
30	H-LD20-n45R2			0.45	2	86.7	41803	3350	
31	H-LD20-n45R25				2.5	87.2	43311	3411	

S-	H-	LD20	Bt17	n30	R15
No mark: CFT S: steel pipe	No Mark: BCR295 H: SA440Mod	l_k/D (20)	B/t_f=17 No mark : B/t_f=25	Axial force ratio n (0.3)	Rotation angle R_0 (1.5%)

5. CFT, Steel hollow tube
6. Strength of steel tube: 400N class steel tube (BCR295), 590N class steel (SA440Mod)

Table 1 shows a list of specimens and the naming rule of the specimens is also described below the table. The number of specimens is 31. In Table 1, No.5 was loaded with R_0=0.5% until 200 cycles and No.19 was loaded with R_0=1% until 100 cycles, however the strength hardly decreased, therefore, the rotation angles of specimen No.5 and No.19 were increased to 0.75% and 1.25%, respectively, and loading was continued. Table 1 shows the compressive strength of concrete ${}_c\sigma_B$ and Young's modulus E_c which is the secant stiffness at $1/3\,{}_c\sigma_B$.

2.2 Specimen and material properties

As for the steel tube, square steel tubes of □-150×6, □-150×9 and welded box-shaped cross section of □-150×6 were used (A mark □ indicates a square-shape). Table 2 shows the mechanical properties of steel materials. In Table 2, ${}_s\sigma_u$ is the tensile strength, ε_y is the yield strain, E_s is the Young's modulus of the steel tube, and F and W are the flange plate and web plate of the SA440Mod steel.

Table 2-The mechanical properties of steel materials

	${}_s\sigma_y$ (N/mm^2)	${}_s\sigma_u$ (N/mm^2)	${}_s\sigma_y/{}_s\sigma_u$	ε_y (%)	E_s (N/mm^2)
□-150×6	378	457	0.84	0.18	2.10×10^5
□-150×9	406	449	0.90	0.19	2.14×10^5
F	479	590	0.81	0.23	2.09×10^5
W	478	589	0.81	0.23	2.08×10^5

2.3 Outline of experimental results

Fig. 2 shows the relationship between lateral load and rotation angle, and Fig. 3 shows the relationship between the lateral load Q_i at the displacement reversal point and the number of cycles obtained by the experimental work [10]. The Q_i is normalized by the maximum lateral load Q_{max}. In previous studies, it is shown that the strength decreased more as the rotation angle and axial force ratio became larger. In this study, limit cycles indicating the reduction of lateral load by 95%, 90%, 85% and 80%, $N_{95\%}$, $N_{90\%}$, $N_{85\%}$, $N_{80\%}$, were defined as an index for exhibiting the performance against strength deterioration of CFT columns.

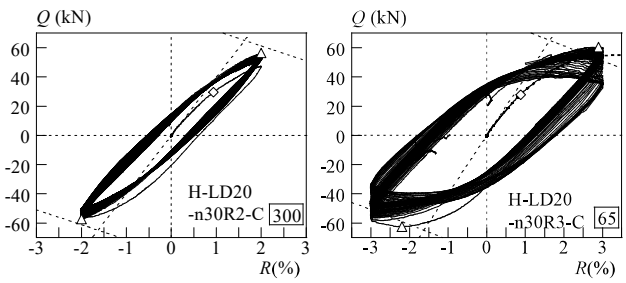

(a) n=0.3, R_0=2% (b) n=0.3, R_0=3%

Fig. 2- Lateral loading- rotation angle relationship

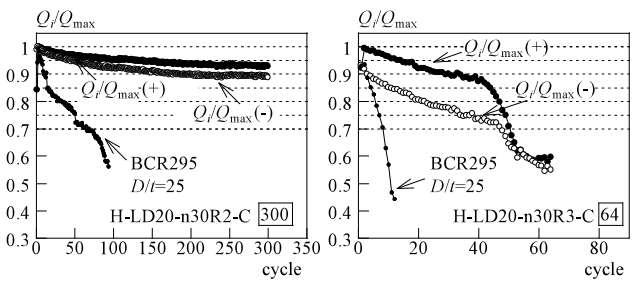

(a) n=0.3, R_0=2% (b) n=0.3, R_0=3%

Fig. 3-Load deterioration

3. Relationship between strength deterioration behavior and unloading stiffness

3.1 Elastic lateral stiffness and unloading stiffness

The elastic lateral stiffness K_e, when the entire cross section is valid and elastic, is calculated by Eq. (1).

$$K_e = \frac{Q}{R_b} = \frac{ZN}{\tan Z - Z} \tag{1}$$

R_b in Eq. (1) is the rotation angle due to bending deformation, $Z = L\sqrt{N / EI}$, $EI=E_cI_c+E_sI_s$. I_c and I_s are the moments of inertia of area of filled concrete and steel tube, calculated as valid for all cross sections.

Fig. 4 shows a schematic diagram of the relationship between lateral load Q and rotation angle R. In this paper, the rotation angle at a reversal point (point B in Fig.4) is called the experienced rotation angle R_0. The rotation angle when the lateral load becomes zero after unloading from the reversal point (point A in Fig.4) is called the residual rotation angle R_r. from the relationship between lateral load and rotation angle obtained from the experiment, the values of the experienced rotation angle R_0 and the residual rotation angle R_r were read. The slope of the straight line connecting the displacement reversal point and the residual rotation angle was defined as the unloading stiffness K_r.

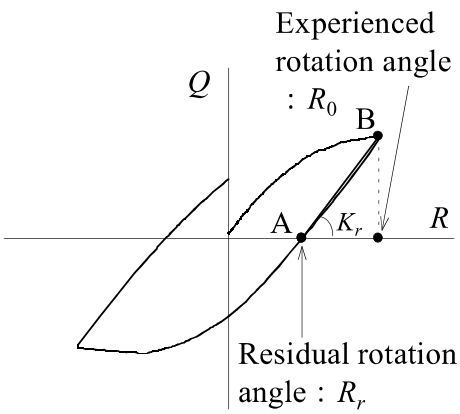

Fig. 4-definition of R_0, R_r and K_r

3.2 Comparison between elastic lateral stiffness and initial lateral stiffness

Fig. 5 shows the comparison between the experimental initial lateral stiffness and the elastic lateral stiffness calculated by Eq. (1). The three kinds of experimental initial lateral stiffness were determined by a slope of a line obtained by connecting the origin and following points.

(1) The point where the rotation angle reaches 0.25% ${}_eK_{exp}$

(2) The point where the strain at the outermost edge of the steel tube reaches the yield strain ${}_yK_{exp}$

(3) The point where the short-term allowable bending moment reaches the primary moment ${}_aK_{exp}$

The short-term allowable strength of (3) is calculated by the simple superposed strength for slender columns shown in Recommendations for CFT Structures [1]. The primary moment is the product of the lateral load Q and the member length L (see Fig.1). In Fig. 5, circle marks indicate ${}_eK_{exp}$, square marks indicate ${}_yK_{exp}$, and triangle marks indicate ${}_aK_{exp}$. And plots for n=0.15, 0.3, 0.45(0.5), and 0.6 are shown in red, white, black, and blue, respectively.

The initial lateral stiffness was smaller than the elastic lateral stiffness except for some test specimens and the value of ${}_eK_{exp}/K_e$, ${}_yK_{exp}/K_e$ and ${}_aK_{exp}/K_e$ were from 0.75 to 1.01, 0.62 to 0.82, and 0.60 to 1.18, respectively. The value of K_{exp}/K_e was almost less than unity, except for ${}_aK_{exp}/K_e$ =1.18 when n=0.6 and

l_k/D=20. This is because that in the case of low axial force such as n =0.15, 0.3, the neutral axis is in the cross section and the concrete does not bear the tensile strength, whereas in the case of high axial force such as n=0.45, 0.5 and 0.6, the neutral axis is outside the cross section and the strain-stress relationship of steel tube and concrete shows non-linearity due to the residual stress of the steel tube and large strain of concrete.

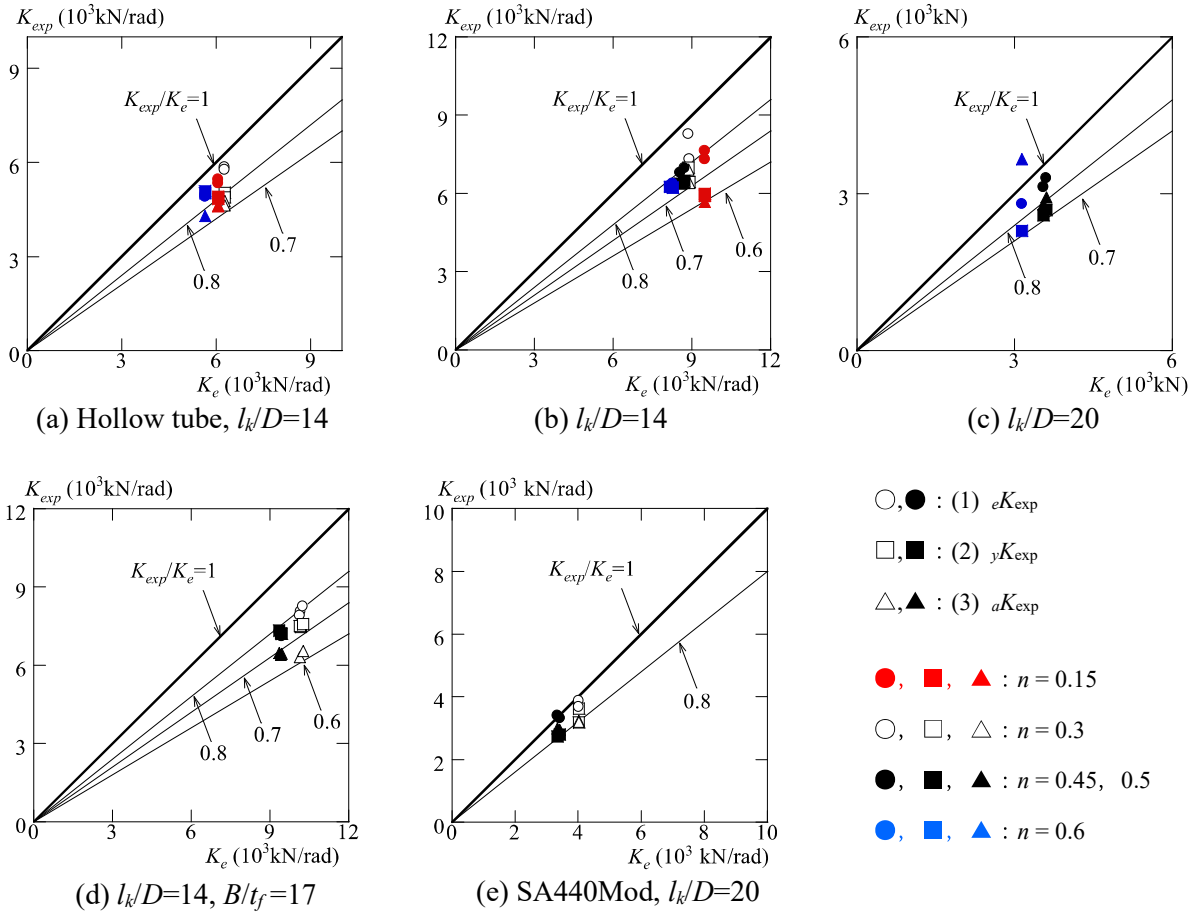

(a) Hollow tube, l_k/D=14 (b) l_k/D=14 (c) l_k/D=20

(d) l_k/D=14, B/t_f=17 (e) SA440Mod, l_k/D=20

Fig. 5- Comparison between the experimental lateral stiffness and the calculated elastic stiffness

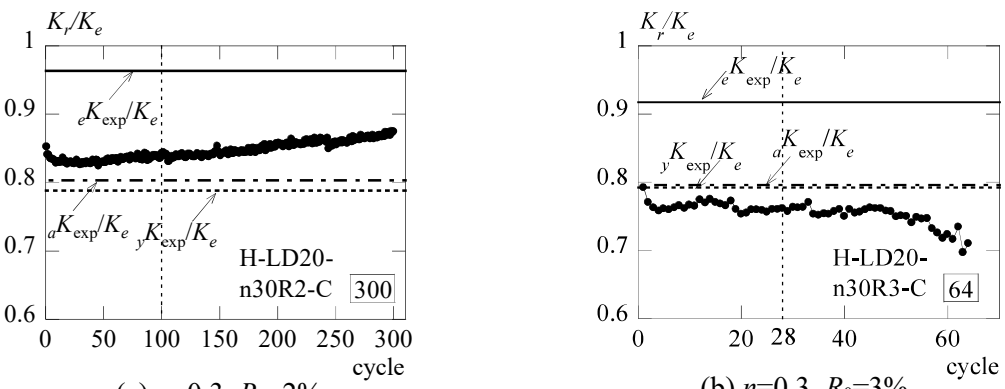

(a) n=0.3, R_0=2% (b) n=0.3, R_0=3%

Fig. 6-Changes in unloading stiffness

(SA440Mod)

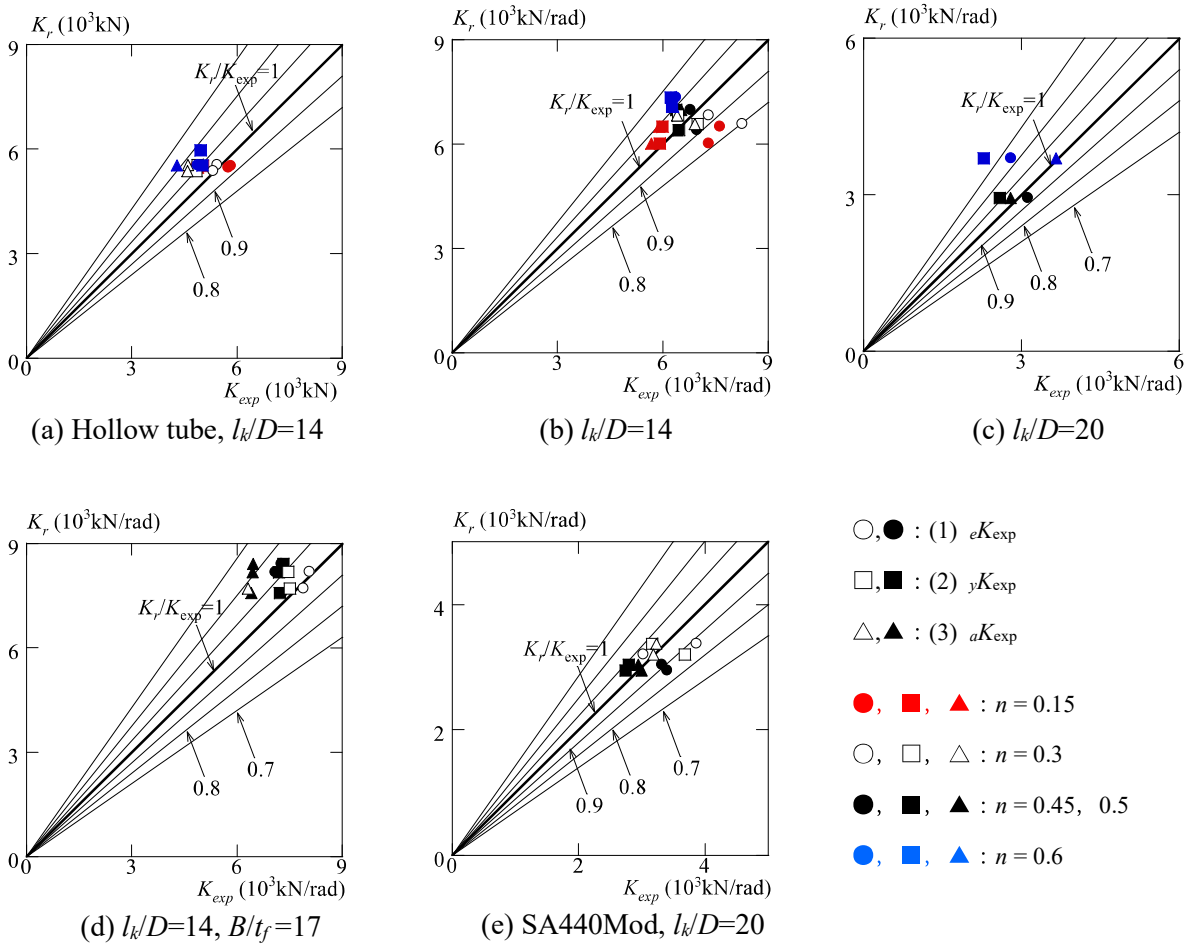

Fig. 7- Comparison between the calculated lateral stiffness and the unloading stiffness

3.3 Relationship between the strength deterioration behavior and unloading stiffness

Fig. 6 shows examples of changes in unloading stiffness of the same specimens shown in Fig. 2 and Fig. 3. According to Fig. 6, unloading stiffness slightly changes when the number of cycles is from the second cycle to the 100 cycles or before the lateral load at the displacement reversal point decreased to 90% of the maximum load. Most of test specimens shows same tendency.

Fig. 7 shows a comparison between the initial lateral stiffness and the unloading stiffness obtained from the experiment. The legend in Fig. 7 is the same as that of Fig. 5. The unloading stiffness at the 100th cycle or at $N_{90\%}$ were used. According to the Fig. 7, the value of unloading stiffness K_r was closest to the value of $_aK_{exp}$ in most of the specimens in B/t_f =25 (Fig. 7 (b), (c) and (e)), closest to the value of $_eK_{exp}$ with B/t_f =17 and n=0.3 specimens (Fig. 7(d)) and hollow steel tube specimens (Fig. 7(a)), and closest to the value of $_yK_{exp}$ with B/t_f =17 and n=0.5 specimens (Fig. 7 (d)). The value of $(K_{exp}-K_r)/K_{exp}$ when the value of K_r/K_{exp} is closest 1 of each specimen are from -15.1% to 4.97%, and test specimens whose value of K_r/K_{exp} are more than 10 % are n=0.5 and 0.6 specimens.

Therefore, the difference between unloading stiffness and initial lateral stiffness is within about 10% until $N_{90\%}$ is reached or 100 cycles, except when n=0.5 or more.

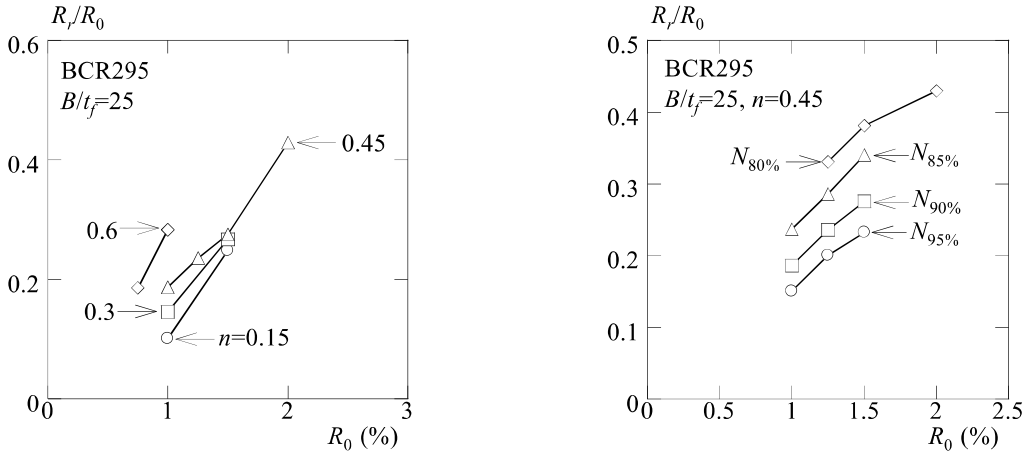

(a) Effect of axial force ratio (b) Effect of limit cycle

Fig. 8-Relationship between R_r/R_0 and R_0

3.4 Relationship between strength deterioration behavior and residual rotation angle

Fig. 8 shows the relationship between the experienced rotation angle R_0 and the residual deformation rate r ($=R_r/R_0$). Fig. 8 (a) and (b) show the R_0-r relationships when axial force ratio n and the limit cycle are taken as parameters, respectively. According to Fig. 8 (a), value of the residual deformation rate r increases as the axial force ratio and experienced rotation angles increase. This tendency was observed in previous research which used the incremental displacement cyclic lateral loading test results [6]. According to Fig. 8 (b), as for the limit cycle, the value of r increased in the following order: $N_{95\%}$, $N_{90\%}$, $N_{85\%}$, and $N_{80\%}$.

4. Conclusions

In this study, the relationship between the strength deterioration behaviour of CFT long columns and the unloading stiffness K_r and residual rotation angle R_r were examined by using the previous experimental study. A limit cycle indicating the reduction of lateral load was defined as an index for exhibiting the performance against strength deterioration. The findings obtained are shown below.

(1) The initial lateral stiffness K_{exp} is smaller than the calculated elastic lateral stiffness K_e, and the ratio between initial lateral stiffness and elastic lateral stiffness K_{exp}/K_e was 0.60 to 1.01 with one exception.

(2) Except when the axial force ratio n equals to 0.5 or more, the difference between unloading stiffness K_r and initial lateral stiffness K_{exp} was within about 10% until the limit cycle $N_{90\%}$ was reached.

(3) The ratio between the residual rotation angle R_r and the experienced rotation angle R_0 defined as the residual deformation rate $r=R_r/R_0$ increased as the axial force ratio increased. Furthermore, considering the limit cycles, the value of r increased in the following order: $N_{95\%}$, $N_{90\%}$, $N_{85\%}$, and $N_{80\%}$.

Acknowledgement

This study was supported by the Grant-in-Aid for Scientific Research of Japan Society for the Promotion of Science.

References

[1] Architectural Institute of Japan (2008): R*ecommendations for design and construction of concrete filled steel tubular structures* (in Japanese)

[2] Yoshida, K., Kido, M., Tsuda, K. (2005): Study on initial stiffness of square CFT columns subjected to horizontal and constant axial forces, *Proc. of constructional steel*, Vol.23, pp.778-783 (in Japanese)

[3] Handa, R., Kido, M., Tsuda, K. (2016): Effect of strain-stress relationship of steel tube on the initial stiffness of square CFT columns, *Proc. of constructional steel*, Vol.24, pp.87-94 (in Japanese)

[4] Nakamura, G., Fujinaga, T., Mitani, I. and Ohtani, Y. (2003): Model for the skeleton curve of square CFT beam-columns, *Concrete Research and Technology*, Vol.14, No.2 (in Japanese)

[5] Varma, A.H., Ricles, J.M., Sause, R., and Lu, L.W (2004): Seismic behavior and design of high-strength square concrete-filled steel tube beam columns, ASCE Journal of Engineering Vol. 130 No.2, pp.169-179

[6] Kido, M., Tsuda, K. (2005): Relation between experimental lateral drift angle and residual one of concrete filled steel square tubular columns, *Proc. of constructional steel*, Vol.13, pp.503-508 (in Japanese)

[7] Jyozaki, K., Kido, M. (2018): Hysteresis characteristics of square CFT columns subjected to axial force and bending moment, Streamlining Information Transfer between Construction and Structural Engineering, Proc. of ASEA-SEC4, pp.ST43-1-6

[8] Kido, M., Tsuda, K., Fukumoto, T., Ichinohe, Y., Morita, K. (2019): Behavior of square concrete filled steel tube beam-columns subjected to lateral load with constant cyclic displacement, *Journal of Structural and Construction Engineering (Transactions of AIJ)*, Vol.84, No.759, pp.725-735 (in Japanese)

[9] Kido, M., Tsuda, K., Fukumoto, T., Ichinohe, Y., Morita, K. (2020): Limit cycle of square concrete filled steel tubular beam-columns subjected to lateral load with constant cyclic displacement, *Journal of Structural and Construction Engineering (Transactions of AIJ)*, Vol.85, No.773, pp.981-991 (in Japanese)

[10] Jyozaki, K., Kido, M., Iketaka, M., CUI, G., Susuki, T. (2020): Structural performance of square CFT columns using 590N class steel under cyclic lateral loading with constant deflection, Part1, Part2, *AIJ Kyushu Chapter Architectural Research Meeting*, No.59, pp.289-296 (in Japanese)

[11] Susuki, T., Kido, M. (2020): Relation between strength deterioration behavior and unloading stiffness of square CFT columns under cyclic lateral loading, *Proc. of constructional steel*, Vol.28, pp.909-916 (in Japanese)

